ISSN 1392 - 1207. MECHANIKA. 2012 Volume 18(3): 292-300

Electro elastic analysis of a pressurized thick-walled functionally graded piezoelectric cylinder using the first order shear deformation theory and energy method

G.H. Rahimi, M. Arefi, M.J. Khoshgoftar
Department of Mechanical Engineering, Tarbiat Modares University, Tehran, Iran, Email: rahimi_gh@modares.ac.ir
crossref http://dx.doi.org/10.5755/j01.mech.18.3.1875

1. Introduction

Piezoelectrics are new groups of material which can be used as a sensor or actuator in electromechanical systems. These materials can exchange the mechanical deformations into electric potential. Conversely, the electric potential can be exchanged to the mechanical deformation. The piezoelectric sensors or actuators may be designed as many structural elements such as beam, plate or cylindrical shell. The piezoelectric analysis of a functionally graded piezoelectric (FGP) cylindrical pressure vessel is studied in the present paper. A brief review of functionally graded material (FGM) and functionally graded piezoelectric material (FGPM) are performed in introduction.

One of the most applicable structures in the mechanical engineering is the shells. In this study, the cylindrical shell structure is considered. Lame [1] studied the exact solution of a thick walled cylinder under inner and outer pressures. It was supposed the cylinder to be axisymmetric and isotropic. Piezoelectric property has been discovered by Pierre and Jacques Curie in Paris (1888). Shear deformation theory has been proposed by Naghdi and Cooper [2]. The application of first order shear deformation theory for an isotropic cylinder has been proposed by Mirsky and Hermann [3]. In the 1980's one Japanese group of material scientists created new class of materials. Properties of this material are varying continuously and gradually in terms of coordinate system components.

The researches on the thermal and vibration analysis of functionally graded materials have been started in the first years of decade 1990 [4]. Displacement and stress analysis of a functionally graded cylinder under the thermal and mechanical loads is performed analytically by Jabbari et al [5]. It was supposed the material properties are varying as a power function in terms of radial coordinate system. Chen et al [6] investigated the mechanical and electrical analyses of a spherical shell. Liu et al [7] proposed an analytical model for free vibration analysis of a cylindrical shell under mechanical and electrical loads. Mindlin's theory is investigated for this analysis and a sinusoidal function is used for simulation of the electric potential distribution. Wu, Jiang and Liu [8] investigated the elastic stability of a FG cylinder. They employed the shell Donnell's theory to derive the strain-deformation relations. Exact solution of a FGP clamped beam is investigated by Shi and Chen [9]. Peng-Fei and Andrew [10] studied the piezoelectric analysis of a cylindrical shell. Lu et al [11] studied the exact solution of a FGP cylinder under bending. Dai et al [12] analyzed the electromagnetoelastic behavior of FGP cylindrical and spherical pressure vessels. Babaei and Chen [13] presented exact solution of an infinitely long magneto elastic hollow cylinder and solid rotating cylinder that is polarized and magnetized radially. They supposed the cylinder to be orthotropic and investigated the effect of angular velocity on the hoop and radial stresses. Jabbari et al [14] investigated the thermoelastic behavior of a FG cylinder under the thermal and mechanical loads. Khoshgoftar et al [15] investigated the thermoelastic analysis of a FGP cylindrical pressure vessel. They supposed that all mechanical and electrical properties are varying as a power function. This mentioned work was the last comprehensive thermoelastic analysis of a FGP cylindrical shell using the plane elasticity theory. The present paper develops the previous paper significantly using the shear deformation theory and proposes an analytical formulation for a comprehensive analysis of a FGP cylinder. The proposed formulation is validated at the regions that are adequate far from two ends of the cylinder with the previous plane elasticity theory. Thermo-elastic analysis of a functionally graded cylinder is investigated analytically by Arefi and Rahimi [16]. They used the first order shear deformation theory (FSDT) for thermoelastic analysis of a FG structure. The achieved results are compared with those results that have been derived using the plane elasticity theory. Thermoelastic vibration and buckling characteristics of a functionally graded piezoelectric cylindrical shell is investigated analytically by Sheng and Wang [17, 18]. First order shear deformation theory is investigated for simulation of the deformations in structure. Electric potential is considered as a quadratic function along the thickness. The Hamilton's principle and Maxwell's equation are considered for solution of the problem. The critical values of axial load, temperature and voltage are investigated for different boundary conditions. Analytical solution for electromagneto thermoelastic behaviors of a functionally graded piezoelectric hollow cylinder under a uniform magnetic field and subjected to thermoelectromechanical loads is investigated by Dai et al [19]. They presented advantageous of material non homogeneity for design optimization of electro mechanical structures and systems.

As mentioned in the literature, there is not reported a comprehensive analysis about electroelastic analysis of a FGP structure by considering the whole nonzero piezoelectric coefficient and in the general state (last study devoted to Dai et al [19] that the cylinder is analyzed using one dimensional method. The proposed method in that paper has not ability to consider other components of strain and piezoelectric coefficients). Therefore, the present paper employs the comprehensive electroelastic formulation for the analysis of a FGP cylinder under inner pressure as

an applied problem. The whole elastic, piezoelectric and dielectric coefficients in constitutive and Maxwell's equations are considered to be nonzero. This subject has been disregarded in the previous papers [15, 19]. Although the mentioned problem at the end of the paper can be considered as a plane strain problem, the present method of solution has enough capability to solve the problem in the general state with considering the whole piezoelectric coefficients. This advantageous condition can not be understood in the plane strain method.

2. Formulation

In the present paper, the FSDT is employed to simulate the deformations. Based on this theory, deformation of every layer of the cylinder is decomposed into deformation of the middle surface and rotation about outward axis of the middle surface [3]. In order to better understand this theory, it is necessary to expand Lame's solution for a cylindrical pressure vessel. Based on the Lame's theory, symmetrical distribution of the radial displacement u may be obtained as follows [16, 20-24]

$$u = c_1 r + \frac{c_2}{r} \tag{1}$$

where r is the radius of every layer of the cylinder. In the general state, this distance can be obtained in terms of the radius of middle surface R and distance of every layer with respect to middle surface ρ. By substitution of r into Lame's solution (Eq. (1)) and applying the Taylor expansion, Eq. (1) may be obtained as a function of ρ as follows [16]

$$r = R+\rho \;\rightarrow u = c_1\left(R+\rho\right) + \frac{c_2}{R+\rho} = c_0' + c_1'\rho + ... + c_m'\rho^m \tag{2}$$

This formulation (Eq. (2)) is known as the shear deformation theory (SDT). By setting m = 1, the first order shear deformation theory is employed for the analysis. Based on this theory, every deformation component can be stated by two variables including the rotation and displacement. For a symmetric cylindrical shell, the radial and axial components of deformation may be considered as follows [16]

$$u_z = u + \rho\psi_z = w + \rho\psi_r \tag{3}$$

where u_z , w_r are the axial and radial components of deformation, respectively, u, w, ψ_z, ψ_r are only functions of the axial component of coordinate system (z). By considering Eq. (3), the strain components are

$$\begin{cases} \varepsilon_r = \dfrac{\partial w_r}{\partial \rho} = \psi_r \\ \varepsilon_\theta = \dfrac{w_r}{r} = \dfrac{w + \rho\psi_r}{R+\rho} \\ \varepsilon_z = \dfrac{\partial u_z}{\partial z} = \dfrac{\partial u}{\partial z} + \rho\dfrac{\partial \psi_z}{\partial z} \\ \gamma_{rz} = 2\times\varepsilon_{rz} = \dfrac{\partial u_z}{\partial \rho} + \dfrac{\partial w_r}{\partial z} = \psi_z + \dfrac{\partial w}{\partial z} + \rho\dfrac{\partial \psi_r}{\partial z} \end{cases} \tag{4}$$

The previous papers did not consider the piezoelectric structure in comprehensive condition and by considering the whole piezoelectric coefficients. The present paper improves the previous incompleteness and considers a FGP cylindrical shell in complete conditions. Therefore, stress-strain relations are [15]

$$\sigma_{ij} = \sigma_{ij})_m + \sigma_{ij})_e = C_{ijkl}\varepsilon_{kl} - e_{ijk}E_k \rightarrow \begin{Bmatrix} \sigma_{rr} = C_{rrzz}\varepsilon_{zz} + C_{rrrr}\varepsilon_{rr} + C_{rr\theta\theta}\varepsilon_{\theta\theta} - e_{rrz}E_z - e_{rr\theta}E_\theta - e_{zzr}E_r \\ \sigma_{\theta\theta} = C_{\theta\theta zz}\varepsilon_{zz} + C_{\theta\theta rr}\varepsilon_{rr} + C_{\theta\theta\theta\theta}\varepsilon_{\theta\theta} - e_{\theta\theta z}E_z - e_{\theta\theta\theta}E_\theta - e_{\theta\theta r}E_r \\ \sigma_{zz} = C_{zzzz}\varepsilon_{zz} + C_{zzrr}\varepsilon_{rr} + C_{zz\theta\theta}\varepsilon_{\theta\theta} - e_{zzz}E_z - e_{zz\theta}E_\theta - e_{zzr}E_r \\ \sigma_{rz} = C_{rzrz}\varepsilon_{rz} \end{Bmatrix} \tag{5}$$

where C_{ijkl}, e_{ijk} are elastic stiffness and piezoelectric coefficients, E_k is electric field component. Based on Eq. (5), the electric field has no effect on the shear stress. By having the components of the electric field, Eq. (5) can be completed. Electric field is equal to negative divergence of the electric potential. The electric field vector is in accordance with direction of decreasing of the electric potential.

$$\vec{E} = -\vec{\nabla}\phi \rightarrow \left\{E_r, E_\theta, E_z\right\} = -\left\{\frac{\partial\phi}{\partial r}, \frac{1}{r}\frac{\partial\phi}{\partial\theta}, \frac{\partial\phi}{\partial z}\right\} \tag{6}$$

where ϕ is the electric potential function. Due to the symmetric condition of the problem (symmetric loading, boundary conditions and material properties), Eq. (6) can be reduced using $\frac{\partial}{\partial r} = \frac{\partial}{\partial \rho}$ as follows

$$E_r = -\frac{\partial\phi}{\partial\rho},\; E_\theta = 0,\; E_z = -\frac{\partial\phi}{\partial z} \tag{7}$$

Based on the results of the previous papers [15, 17, 18] the electric potential function may be supposed as a quadratic function in the radial direction and an unknown function in the longitudinal direction

$$\phi(z,\rho) = \phi_0(z) + \rho\phi_1(z) + \rho^2\phi_2(z) \tag{8}$$

By substitution of Eq. (8) into Eq. (7), the electric field (Eq. (6)) can be reduced to

$$\vec{E} = -\left\{\phi_1(z) + 2\rho\phi_2(z), 0, \frac{\partial\phi_0}{\partial z} + \rho\frac{\partial\phi_1}{\partial z} + \rho^2\frac{\partial\phi_2}{\partial z}\right\} \tag{9}$$

The electric displacement may be obtained as a linear combination of the strain and electric field as follows [17, 18]

$$D_i = e_{ijk}\varepsilon_{jk} + \eta_{ik}E_k \rightarrow \begin{Bmatrix} D_r = e_{rzz}\varepsilon_z + e_{rrr}\varepsilon_r + e_{r\theta\theta}\varepsilon_\theta + \eta_{rz}E_z + \eta_{rr}E_r \\ D_\theta = e_{\theta zz}\varepsilon_z + e_{\theta rr}\varepsilon_r + e_{\theta\theta\theta}\varepsilon_\theta + \eta_{\theta z}E_z + \eta_{\theta r}E_r \\ D_z = e_{zzz}\varepsilon_z + e_{zzr}\varepsilon_r + e_{z\theta\theta}\varepsilon_\theta + \eta_{zz}E_z + \eta_{zr}E_r \end{Bmatrix} \quad (10)$$

where η_{ik} are dielectric coefficient. By having the components of the stresses, strains, electric field and electric displacements (Eqs. (4), (5), (9) and (10)), the energy equation per unit volume may be obtained. Total energy includes the mechanical and electrical energy. Mechanical energy is equal to one half of multiplying the stress tensor in the corresponding strain tensor. Electrical energy is equal to one half of multiplying the electric displacement tensor in the corresponding electric field tensor. Therefore, energy per unit volume ($\bar{u}$) may be obtained as follows

$$\begin{aligned} \bar{u} &= \frac{1}{2}\left[\{\varepsilon\}^T\{\sigma\} - \{E\}^T\{D\}\right] = \\ &= \frac{1}{2}\begin{Bmatrix} \sigma_z\varepsilon_z + \sigma_z\varepsilon_z + \sigma_t\varepsilon_t + \tau_{xz}\gamma_{xz} - \\ -E_xD_x - E_zD_z - E_tD_t \end{Bmatrix} = \\ &= \frac{1}{2}\left[C_{rrzz}\varepsilon_{zz} + C_{rrrr}\varepsilon_{rr} + C_{rr\theta\theta}\varepsilon_{\theta\theta} - e_{rrz}E_z - e_{zzr}E_r\right]\varepsilon_r + \\ &+\left[C_{\theta\theta zz}\varepsilon_{zz} + C_{\theta\theta rr}\varepsilon_{rr} + C_{\theta\theta\theta\theta}\varepsilon_{\theta\theta} - e_{\theta\theta z}E_z - e_{\theta\theta r}E_r\right]\varepsilon_\theta + \\ &+\left[C_{zzzz}\varepsilon_{zz} + C_{zzrr}\varepsilon_{rr} + C_{zz\theta\theta}\varepsilon_{\theta\theta} - e_{zzz}E_z - e_{zzr}E_r\right]\varepsilon_z + \\ &+\left[C_{rzrz}\gamma_{rz}\right]\gamma_{rz} - \\ &-E_z\left[e_{zzz}\varepsilon_z + e_{zzr}\varepsilon_r + e_{z\theta\theta}\varepsilon_\theta + \eta_{zz}E_z + \eta_{zr}E_r\right] - \\ &-E_r\left[e_{rzz}\varepsilon_z + e_{rrr}\varepsilon_r + e_{r\theta\theta}\varepsilon_\theta + \eta_{rz}E_z + \eta_{rr}E_r\right] \end{aligned} \quad (11)$$

The total energy must be evaluated by integration of Eq. (11) on the volume of the cylinder. The volume element of the cylinder is $2\pi(R+z)dzdx$. Therefore, the total energy of the system is

$$\begin{aligned} U &= 2\pi\int_0^L\int_{-\frac{h}{2}}^{\frac{h}{2}}(R+\rho)\bar{u}d\rho dz = \\ &= \int_0^L F_1(u, w, \psi_z, \psi_r, \phi_0, \phi_1, \phi_2, z)dz \end{aligned} \quad (12)$$

where $F_1(u, w, \psi_z, \psi_r, \phi_0, \phi_1, \phi_2, z)$ is the appropriate functional of the system which can be obtained as follows

$$\frac{F_1}{\pi} = F(u, w, \psi_z, \psi_r, \phi_0, \phi_1, \phi_2, z) = 2\int_{-\frac{h}{2}}^{\frac{h}{2}}\bar{u}(R+\rho)d\rho \quad (13)$$

$F(u, w, \psi_z, \psi_r, \phi_0, \phi_1, \phi_2, z)$ can be decomposed to three types of sentences as follows

$$F(u, w, \psi_z, \psi_r, \phi_0, \phi_1, \phi_2, z) = U_S(z) + U_{\text{Piezo}}(z) - U_{Die}(z) \quad (14)$$

These sentences include strain energy $U_S(z)$, piezoelectric energy $U_{Piezo}(z)$ and dielectric energy $U_{Die}(z)$.

2.1. Calculation of the external works

External works such as pressure [16] or rotational loads [25] can be considered in this section. Energy of internal pressure is equals to multiplying the pressure in the radial deformation of the inner surface of the cylinder. Inner pressure applies in the same direction of the deformation. Eq. (15) indicates work is done by the internal pressure. Fig. 1 shows the schematic figure of the cylindrical pressure vessel.

$$\begin{aligned} W_1 &= \int_0^{2\pi}\int_0^l + P_i\left(w_{z=-h/2}\right)dzd\theta = \\ &= \int_0^{2\pi}\int_0^l + P_i\left(R-\frac{h}{2}\right)\left(w-\frac{h}{2}\psi_r\right)dzd\theta \rightarrow \frac{W_1}{\pi} = \\ &= 2\int_0^l P_i\left(R-\frac{h}{2}\right)wdz + 2\int_0^l\frac{h}{2}\left(-P_i\left(R-\frac{h}{2}\right)\right)\psi_r dz = \\ &= \int_0^l\left[f_1w + f_2\psi_r\right]dz = \int_0^l W_1'dz \\ f_1 &= 2P_i\left(R-\frac{h}{2}\right),\ f_2 = h\left(-P_i\left(R-\frac{h}{2}\right)\right) \end{aligned} \quad (15)$$

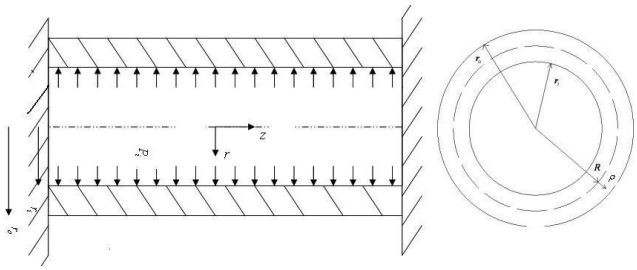

Fig. 1 Schematic figure of a FGP cylinder under internal pressure

2.2. Variation of the energy equation

Total energy of the system is obtained by subtraction of Eq. (15) from Eq. (14) as follows

$$\begin{aligned} &F(u, w, \psi_z, \psi_r, \phi_0, \phi_1, \phi_2, z) = \\ &= U_S(z) + U_{Piezo}(z) - U_{Die}(z) - W_1' \end{aligned} \quad (16)$$

Every terms of above functional $U_S(z)$, $U_{Piezo}(z)$, $U_{Die}(z)$ are demonstrated as follows

$$\begin{aligned} U_S(z) &= \sum_{i=1}^{9}A_i(z)\,f_i(u, w, \psi_x, \psi_z, \phi_0, \phi_1, \phi_2, z) \\ U_{Piezo}(z) &= \sum_{i=1}^{32}C_i(z)\,I_i(u, w, \psi_x, \psi_z, \phi_0, \phi_1, \phi_2, z) \\ U_{Die}(z) &= \sum_{i=1}^{16}D_i(z)\,J_i(u, w, \psi_x, \psi_z, \phi_0, \phi_1, \phi_2, z) \end{aligned} \quad (17)$$

Eq. (16) includes seven functions. By using Euler equation, variation of Eq. (16) can be expressed as follows

$$\frac{\partial F}{\partial Q_i}-\frac{\partial}{\partial x}\left(\frac{\partial F}{\partial\left(\frac{\partial Q_i}{\partial x}\right)}\right)=0,\quad Q_i=u,w,\psi_z,\psi_r,\phi_0,\phi_1,\phi_2 \qquad (18)$$

Using the Euler equation, final governing differential equation of the system in matrix form is

$$\left.\begin{aligned}&[G_1]_{7\times7}\frac{d^2}{dz^2}\{X\}+[G_2]_{7\times7}\frac{d}{dz}\{X\}+[G_3]_{7\times7}\{X\}=\{F\}_{7\times1}\\&\{X\}=\{u\ w\ \psi_z\ \ \psi_r\ \ \phi_0\ \ \phi_1\ \ \phi_2\}^T\end{aligned}\right\} \qquad (19)$$

where matrices G_i, F are functions of A_i, C_i, D_i that are demonstrated earlier in Eq. (17). The complete set of partial differential equations for a functionally graded piezoelectric shell of revolution with variable thickness and curvature can be studied in future work of authors [26]. The functions of A_i, C_i, D_i are demonstrated as follows

$$A_1(z)=\int_{-\frac{h}{2}}^{\frac{h}{2}}(R+\rho)C_{zzzz}d\rho,\quad A_2(z)=\int_{-\frac{h}{2}}^{\frac{h}{2}}\rho(R+\rho)C_{zzzz}d\rho,\quad A_3(z)=\int_{-\frac{h}{2}}^{\frac{h}{2}}\rho^2(R+\rho)C_{zzzz}d\rho,\quad A_4(z)=\int_{-\frac{h}{2}}^{\frac{h}{2}}C_{zz\theta\theta}d\rho,$$

$$A_5(z)=\int_{-\frac{h}{2}}^{\frac{h}{2}}\rho C_{zz\theta\theta}d\rho,\quad A_6(z)=\int_{-\frac{h}{2}}^{\frac{h}{2}}\rho^2C_{zz\theta\theta}d\rho,\quad A_7(z)=\int_{-\frac{h}{2}}^{\frac{h}{2}}(R+\rho)C_{zzrr}d\rho,\quad A_8(z)=\int_{-\frac{h}{2}}^{\frac{h}{2}}\rho(R+\rho)C_{zzrr}d\rho,$$

$$A_9(z)=\int_{-\frac{h}{2}}^{\frac{h}{2}}C_{zz\theta\theta}d\rho,\quad A_{10}(z)=\int_{-\frac{h}{2}}^{\frac{h}{2}}\rho C_{rr\theta\theta}d\rho,\quad A_{11}(z)=\int_{-\frac{h}{2}}^{\frac{h}{2}}\frac{C_{\theta\theta\theta\theta}}{R+\rho}d\rho,\quad A_{12}(z)=\int_{-\frac{h}{2}}^{\frac{h}{2}}\frac{\rho C_{\theta\theta\theta\theta}}{R+\rho}d\rho,\quad A_{13}(z)=\int_{-\frac{h}{2}}^{\frac{h}{2}}\frac{\rho^2C_{\theta\theta\theta\theta}}{R+\rho}d\rho,$$

$$A_{14}(z)=\int_{-\frac{h}{2}}^{\frac{h}{2}}(R+\rho)C_{rrrr}d\rho,\quad A_{15}(z)=\int_{-\frac{h}{2}}^{\frac{h}{2}}C_{rzrz}(R+\rho)d\rho,\quad A_{16}(z)=\int_{-\frac{h}{2}}^{\frac{h}{2}}\rho C_{rzrz}(R+\rho)d\rho,\quad A_{17}(z)=\int_{-\frac{h}{2}}^{\frac{h}{2}}\rho^2C_{rzrz}(R+\rho)d\rho.$$

$$C_1=\int_{-\frac{h}{2}}^{\frac{h}{2}}e_{zzz}(R+\rho)d\rho],\quad C_2=\int_{-\frac{h}{2}}^{\frac{h}{2}}ze_{zzz}(R+\rho)d\rho,\quad C_3=\int_{-\frac{h}{2}}^{\frac{h}{2}}\rho^2e_{zzz}(R+\rho)d\rho,\quad C_4=\int_{-\frac{h}{2}}^{\frac{h}{2}}\rho^3e_{zzz}(R+\rho)d\rho,$$

$$C_5=\int_{-\frac{h}{2}}^{\frac{h}{2}}e_{rrr}(R+\rho)d\rho,\quad C_6=\int_{-\frac{h}{2}}^{\frac{h}{2}}e_{rrr}\rho(R+\rho)d\rho,\quad C_7=\int_{-\frac{h}{2}}^{\frac{h}{2}}e_{zzr}(R+\rho)d\rho,\quad C_8=\int_{-\frac{h}{2}}^{\frac{h}{2}}e_{zzr}\rho(R+\rho)d\rho,$$

$$C_9=\int_{-\frac{h}{2}}^{\frac{h}{2}}e_{zzr}\rho^2(R+\rho)d\rho,\quad C_{10}=\int_{-\frac{h}{2}}^{\frac{h}{2}}e_{rzz}(R+\rho)d\rho,\quad C_{11}=\int_{-\frac{h}{2}}^{\frac{h}{2}}e_{rzz}\rho(R+\rho)d\rho,\quad C_{12}=\int_{-\frac{h}{2}}^{\frac{h}{2}}e_{rzz}(R+\rho)\rho^2d\rho,$$

$$C_{13}=\int_{-\frac{h}{2}}^{\frac{h}{2}}e_{rrz}(R+\rho)d\rho,\quad C_{14}=\int_{-\frac{h}{2}}^{\frac{h}{2}}e_{rrz}\rho(R+\rho)d\rho,\quad C_{15}=\int_{-\frac{h}{2}}^{\frac{h}{2}}e_{rrz}(R+\rho)\rho^2d\rho,\quad C_{16}=\int_{-\frac{h}{2}}^{\frac{h}{2}}e_{zrr}(R+\rho)d\rho,$$

$$C_{17}=\int_{-\frac{h}{2}}^{\frac{h}{2}}e_{zrr}\rho(R+\rho)d\rho,\quad C_{18}=\int_{-\frac{h}{2}}^{\frac{h}{2}}e_{zrr}(R+\rho)\rho^2d\rho,\quad C_{19}=\int_{-\frac{h}{2}}^{\frac{h}{2}}e_{\theta\theta z}d\rho,\quad C_{20}=\int_{-\frac{h}{2}}^{\frac{h}{2}}e_{\theta\theta z}\rho d\rho,\quad C_{21}=\int_{-\frac{h}{2}}^{\frac{h}{2}}e_{\theta\theta z}\rho^2d\rho,$$

$$C_{22}=\int_{-\frac{h}{2}}^{\frac{h}{2}}e_{\theta\theta z}\rho^3d\rho,\quad C_{23}=\int_{-\frac{h}{2}}^{\frac{h}{2}}e_{z\theta\theta}d\rho,\quad C_{24}=\int_{-\frac{h}{2}}^{\frac{h}{2}}e_{z\theta\theta}\rho d\rho,\quad C_{25}=\int_{-\frac{h}{2}}^{\frac{h}{2}}e_{z\theta\theta}\rho^2d\rho,\quad C_{26}=\int_{-\frac{h}{2}}^{\frac{h}{2}}e_{z\theta\theta}\rho^3d\rho$$

$$C_{27}=\int_{-\frac{h}{2}}^{\frac{h}{2}}e_{\theta\theta r}d\rho,\quad C_{28}=\int_{-\frac{h}{2}}^{\frac{h}{2}}e_{\theta\theta r}\rho d\rho,\quad C_{29}=\int_{-\frac{h}{2}}^{\frac{h}{2}}e_{\theta\theta r}\rho^2d\rho,\quad C_{30}=\int_{-\frac{h}{2}}^{\frac{h}{2}}e_{r\theta\theta}d\rho,\quad C_{31}=\int_{-\frac{h}{2}}^{\frac{h}{2}}e_{r\theta\theta}\rho d\rho,\quad C_{32}=\int_{-\frac{h}{2}}^{\frac{h}{2}}e_{r\theta\theta}\rho^2d\rho.$$

$$D_1=\int_{-\frac{h}{2}}^{\frac{h}{2}}\eta_{zz}(R+\rho)d\rho,\quad D_2=\int_{-\frac{h}{2}}^{\frac{h}{2}}\eta_{zz}\rho(R+\rho)d\rho,\quad D_3=\int_{-\frac{h}{2}}^{\frac{h}{2}}\eta_{zz}\rho^2(R+\rho)d\rho,\quad D_4=\int_{-\frac{h}{2}}^{\frac{h}{2}}\eta_{zz}\rho^3(R+\rho)d\rho,$$

$$D_5=\int_{-\frac{h}{2}}^{\frac{h}{2}}\eta_{zz}\rho^4\left(R+\rho\right)d\rho,\quad D_6=\int_{-\frac{h}{2}}^{\frac{h}{2}}\eta_{zr}\left(R+\rho\right)d\rho,\quad D_7=\int_{-\frac{h}{2}}^{\frac{h}{2}}\eta_{zr}\rho\left(R+\rho\right)d\rho,\quad D_8=\int_{-\frac{h}{2}}^{\frac{h}{2}}\eta_{zr}\rho^2\left(R+\rho\right)d\rho,$$

$$D_9=\int_{-\frac{h}{2}}^{\frac{h}{2}}\eta_{zr}\rho^3\left(R+\rho\right)d\rho,\quad D_{10}=\int_{-\frac{h}{2}}^{\frac{h}{2}}\eta_{rz}\left(R+\rho\right)d\rho,\quad D_{11}=\int_{-\frac{h}{2}}^{\frac{h}{2}}\eta_{rz}\rho\left(R+\rho\right)d\rho,\quad D_{12}=\int_{-\frac{h}{2}}^{\frac{h}{2}}\eta_{rz}\rho^2\left(R+\rho\right)d\rho,$$

$$D_{13}=\int_{-\frac{h}{2}}^{\frac{h}{2}}\eta_{rz}\rho^3\left(R+\rho\right)d\rho,\quad D_{14}=\int_{-\frac{h}{2}}^{\frac{h}{2}}\eta_{rr}\left(R+\rho\right)d\rho,\quad D_{15}=\int_{-\frac{h}{2}}^{\frac{h}{2}}\eta_{rr}\rho\left(R+\rho\right)d\rho,\quad D_{16}=\int_{-\frac{h}{2}}^{\frac{h}{2}}\eta_{rr}\rho^2\left(R+\rho\right)d\rho$$

Matrix F has two nonzero components as follows

$$F_{3,1}=2P_i\left(R-\frac{h}{2}\right),\quad F_{4,1}=-2\frac{h}{2}P_i\left(R-\frac{h}{2}\right)$$

3. Solution of the problem

For analysis of the problem and comparing the results of the present method with plane elasticity theory (PET), the solution of the problem must be evaluated at the regions that are adequate far from two ends of the cylinder. This solution is evaluated using Eq. (19) as follows

$$\left[G_3\right]\left\{X\right\}=\left\{F\right\},\ \left\{X\right\}=\left\{u\ \psi_x\ w\ \psi_z\ \phi_0\ \phi_1\ \phi_2\right\}^T \quad (20)$$

The above formulation is used to evaluate the validity of the present method (first order shear deformation theory).

The numerical value of the physical parameters is selected as follows [15]

$$\left.\begin{aligned}
&r_i=0.6\left(\mathrm{m}\right),\ r_o=1\left(\mathrm{m}\right),\ R=0.8\left(\mathrm{m}\right),\\
&C_{zzzz}=79.2\mathrm{GPa},\ C_{zzrr}=C_{rrzz}=45.2\mathrm{GPa},\\
&C_{rrrr}=83.6\mathrm{GPa},\ C_{rr\theta\theta}=C_{\theta\theta rr}=39.3\mathrm{GPa},\\
&C_{zz\theta\theta}=C_{\theta\theta zz}=45.2\mathrm{GPa},\ C_{\theta\theta\theta\theta}=74.1\mathrm{GPa},\\
&C_{zrzr}=79\mathrm{GPa},\ e_{rrr}=0.347\left(\mathrm{VmN}^{-1}\right),\\
&e_{zzr}=e_{rzz}=-0.16\left(\mathrm{VmN}^{-1}\right),\\
&e_{\theta\theta r}=e_{r\theta\theta}=-0.16\left(\mathrm{VmN}^{-1}\right),\\
&\eta_{rr}=9\times10^{-11}\left(\mathrm{mN}^{-1}\right)
\end{aligned}\right\} \quad (21)$$

The cylinder is made of functionally graded material that is graded in the radial direction. Therefore the entire properties must be represented as a power function in terms of the radial coordinate.

$$\left.\begin{aligned}
&C_{ijkl}=C_{ijkl})_{r_i}\left(\frac{R+\rho}{r_i}\right)^{n_1},\ e_{klm}=e_{klm})_{r_i}\left(\frac{R+\rho}{r_i}\right)^{n_2},\\
&\eta_{kl}=\eta_{kl})_{r_i}\left(\frac{R+\rho}{r_i}\right)^{n_3}
\end{aligned}\right\} \quad (22)$$

where $C_{ijkl})_{r_i}, e_{klm})_{r_i}, \eta_{kl})_{r_i}$ are the values of the elastic, piezoelectric and dielectric coefficient, respectively, at inner radius of the cylinder.

4. Results

As mentioned earlier, this paper deals with the analysis of a FGP cylinder at regions that are adequate far from two ends of the cylinder. By setting $n_1=n_2=n_3=n$, Fig. 2 shows the radial distribution of the radial displacement along the thickness for five values of nonhomogenous index ($n=0,\pm1,\pm2$).

Fig. 3 shows the radial distribution of the electric potential along the thickness direction for five values of nonhomogenous index under 80 MPa internal pressure.

The calculations indicate that the circumferential and axial stresses are two main components of the stress tensor. The circumferential stress is maximum component of stress tensor. The previous formulation has not ability to evaluate the axial stress [15]. Evaluation of the axial stress indicates that the value of the axial stress is significant and must be considered in design calculations.

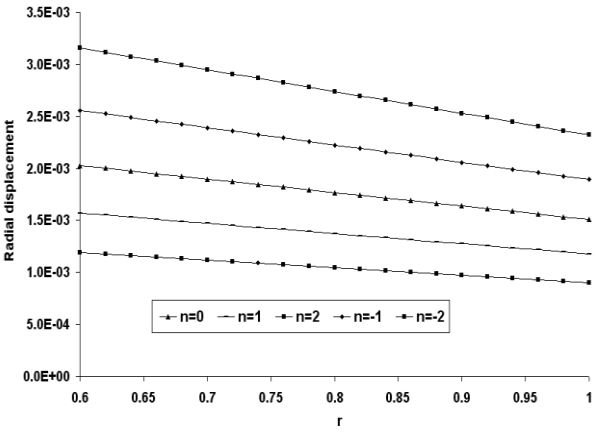

Fig. 2 Radial distribution of the radial displacement along the thickness

Figs. 4 and 5 show the radial distribution of the circumferentialand axial stresses along the thickness direction for five values of nonhomogenous indexes ($n=0,\pm1,\pm2$).

Fig. 4 indicates that the maximum hoop stress is located at inner radius and the minimum of that at outer radius. The decreasing of the stress from inner to outer radii is maximum for n = -2 and this value decreases with increasing the values of nonhomogenous index. n = 2 presents a uniform distribution of stress along the thickness. Fig. 5 is similar to Fig. 4, behaviorally.

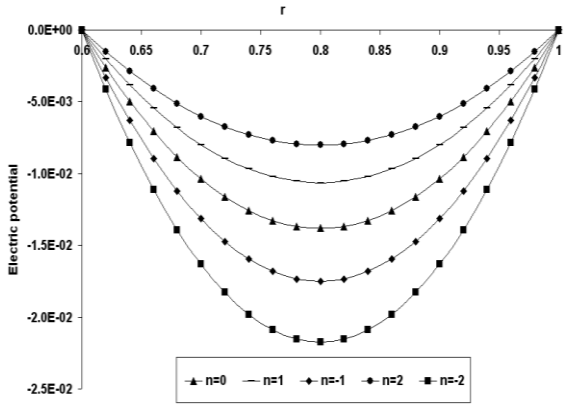

Fig. 3 Radial distribution of the electric potential along the thickness

Figs. 4, 5 indicate that the inner pressure impresses significantly the values of stress at the inner radius rather than the outer radius that pressure is zero. In the other word, the value of stress at the inner radius extremely depends on the value of non homogenous index, while the value of stress at the outer radius weakly depends on the value of nonhomogenous index.

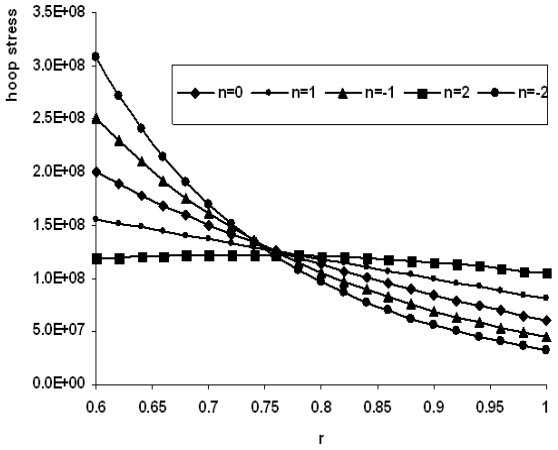

Fig. 4 Radial distribution of the circumferential stress along the thickness

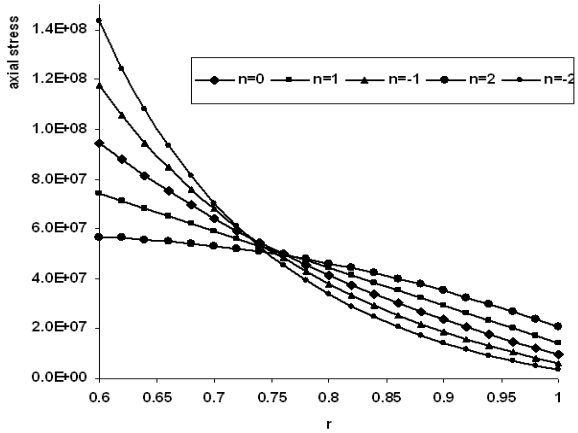

Fig. 5 Radial distribution of the axial stress along the thickness

For validation, it is appropriate to compare these results with whose results that is obtained using the finite element method. Fig. 6 shows comparison between the obtained results using three methods (PET, FSDT and FEM).

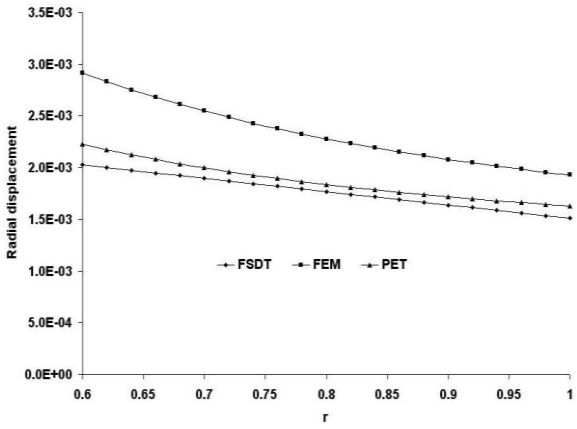

Fig. 6 Comparison between the obtained results with finite element method results

The main objective of this paper is verification of the FSDT results for electro elastic analysis of a FGP cylinder. Figs. 7, 8 show the radial distribution of the radial displacement and electric potential along the thickness direction for five values of nonhomogenous indexes ($n = 0, \pm 1, \pm 2$) based on two theories FSDT and PET. Thick lines represent the value of components based on the plane elasticity theory (PET) and thin lines represent the value of component based on FSDT. The numerical difference between two theories is presented in Tables 1, 2 for radial displacement and electric potential, respectively.

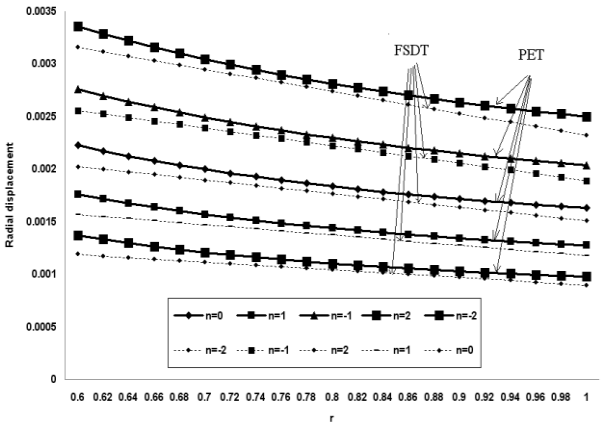

Fig. 7 Comparison between the radial displacement of a FGP cylinder under internal pressure 80 MPa based on two theories (FSDT and PET)

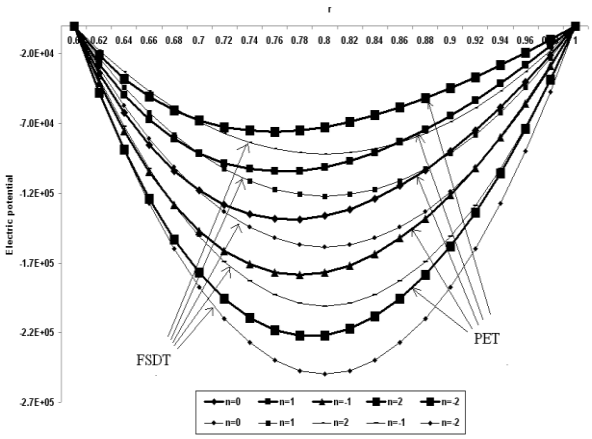

Fig. 8 Comparison between the electric potential of a FGP cylinder under internal pressure 80 MPa based on two theories (FSDT and PET)

Minor difference between two theories arises from the first assumption of the problem. The radial displacement based on the FSDT is considered as a linear function of thickness, while the plane elasticity theory solves the problem using the analytical method and calculation of characteristic equation [15]. In spite of plane elasticity theory, the FSDT has an ability to solve the problem in the two dimensional coordinate systems with appropriate boundary conditions. The plane elasticity theory can present two dimensional responses of a FG cylinder only with simply supported end conditions [14].

Fig. 9 shows the radial distribution of percentage of the difference between radial displacements using two theories. It is observed that the maximum difference is located at the surface of applied pressure. This difference decreases uniformly from the inner radius to the middle of the cylinder, approximately. From the middle surface to the outer surface, the difference increases uniformly.

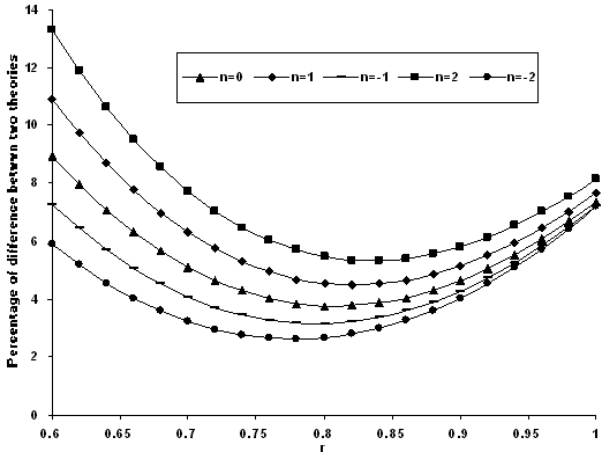

Fig. 9 Percentage of difference between radial displacement using PET and FSDT

5. Discussion and conclusion

Thermoelastic analysis of a FGP cylinder was investigated using the FSDT and energy method in this work. The main results that are concluded from the present paper are classified as follows.

1. The distribution of the radial displacement indicates that the maximum value of the radial displacement is located at the inner radius and the minimum value of the radial displacement is located at the outer radius. This result is accordance with the results of the literature [15].

2. The radial distribution of hoop and axial stresses indicates that the inner pressure impresses significantly the stress at inner radius. This distribution indicates that the value of stress at the inner surface of the cylinder depends strongly on the values of nonhomogenous index. This phenomenon is not repeated at outer surface because of zero outer pressure.

3. The comparison between the PET and FSDT indicates that the present results using FSDT have not significant difference with the results using PET [15]. Especially the radial displacement is strongly in accordance with the results of the plane elasticity theory. This accordance indicates that the first order shear deformation theory has sufficient capability to simulate the displacement with well precision. Therefore the first order shear deformation theory (FSDT) can be employed for the analysis of a functionally graded piezoelectric structure as an excellent theory.

4. Finite element modeling has been performed for simulation of the results that is obtained using the first order shear deformation and plane elasticity theories. The obtained results using FEM justified acceptability of the results using the FSDT and PET.

5. The distribution of the axial stress indicates that this component of stress must be regarded in the design calculation. The value of the axial stress is significant in contrast with the order of the circumferential stress.

Table 1

Comparison between the radial displacements based on two theories

r	ρ	Theories	$n = 0$	$n = 1$	$n = -1$	$n = 2$	$n = -2$
0.6	-0.2	FSDT	0.00203	0.00157	0.00256	0.00119	0.00316
		PET	0.00223	0.00176	0.00276	0.00137	0.00336
0.64	-0.16	FSDT	0.00198	0.00153	0.00249	0.00116	0.00307
		PET	0.00213	0.00168	0.00264	0.00130	0.00322
0.68	-0.12	FSDT	0.00192	0.00149	0.00242	0.00113	0.00299
		PET	0.00204	0.00160	0.00254	0.00124	0.00310
0.72	-0.08	FSDT	0.00187	0.00145	0.00236	0.00110	0.00291
		PET	0.00196	0.00154	0.00245	0.00119	0.00300
0.76	-0.04	FSDT	0.00182	0.00141	0.00229	0.00107	0.00282
		PET	0.00190	0.00149	0.00237	0.00114	0.00290
0.8	0	FSDT	0.00177	0.00137	0.00222	0.00104	0.00274
		PET	0.00184	0.00144	0.00230	0.00110	0.00281
0.84	0.04	FSDT	0.00172	0.00133	0.00216	0.00101	0.00266
		PET	0.00179	0.00140	0.00223	0.00107	0.00274
0.88	0.08	FSDT	0.00166	0.00130	0.00209	0.00098	0.00257
		PET	0.00174	0.00136	0.00218	0.00104	0.00267
0.92	0.12	FSDT	0.00161	0.00126	0.00203	0.00096	0.00249
		PET	0.00170	0.00133	0.00213	0.00102	0.00261
0.96	0.16	FSDT	0.00156	0.00122	0.00196	0.00093	0.00240
		PET	0.00166	0.00130	0.00208	0.00100	0.00255
1	0.2	FSDT	0.00151	0.00118	0.00189	0.00090	0.00232
		PET	0.00163	0.00128	0.00204	0.00098	0.00250

Table 2

Comparison between the electric potentials based on two theories

r	ρ	Theories	$n = 0$	$n = 1$	$n = -1$	$n = 2$	$n = -2$
0.6	-0.2	FSDT	0	0	0	0	0
		PET	0	0	0	0	0
0.64	-0.16	FSDT	-5.7E+04	-4.4E+04	-7.2E+04	-3.3E+04	-9.0E+04
		PET	-6.2E+04	-5.0E+04	-7.6E+04	-3.8E+04	-8.9E+04
0.68	-0.12	FSDT	-1.0E+05	-7.8E+04	-1.3E+05	-5.9E+04	-1.6E+05
		PET	-1.0E+05	-8.1E+04	-1.3E+05	-6.1E+04	-1.5E+05
0.72	-0.08	FSDT	-1.3E+05	-1.0E+05	-1.7E+05	-7.7E+04	-2.1E+05
		PET	-1.3E+05	-9.8E+04	-1.6E+05	-7.3E+04	-2.0E+05
0.76	-0.04	FSDT	-1.5E+05	-1.2E+05	-1.9E+05	-8.8E+04	-2.4E+05
		PET	-1.4E+05	-1.0E+05	-1.8E+05	-7.6E+04	-2.2E+05
0.8	0	FSDT	-1.6E+05	-1.2E+05	-2.0E+05	-9.2E+04	-2.5E+05
		PET	-1.4E+05	-1.0E+05	-1.8E+05	-7.2E+04	-2.2E+05
0.84	0.04	FSDT	-1.5E+05	-1.2E+05	-1.9E+05	-8.8E+04	-2.4E+05
		PET	-1.2E+05	-9.1E+04	-1.6E+05	-6.4E+04	-2.1E+05
0.88	0.08	FSDT	-1.3E+05	-1.0E+05	-1.7E+05	-7.7E+04	-2.1E+05
		PET	-1.0E+05	-7.5E+04	-1.4E+05	-5.2E+04	-1.8E+05
0.92	0.12	FSDT	-1.0E+05	-7.8E+04	-1.3E+05	-5.9E+04	-1.6E+05
		PET	-7.5E+04	-5.3E+04	-1.0E+05	-3.7E+04	-1.3E+05
0.96	0.16	FSDT	-5.7E+04	-4.4E+04	-7.2E+04	-3.3E+04	-9.0E+04
		PET	-4.0E+04	-2.8E+04	-5.5E+04	-1.9E+04	-7.4E+04
1	0.2	FSDT	0	0	0	0	0
		PET	0	0	0	0	0

References

1. **Timoshenko, S.P.** 1976. Strength of Materials: Part II (Advanced Theory and Problems), 3 rd edition, Van Nostrand Reinhold Co, New York.
2. **Naghdi, P.M.; Cooper, R.M.** 1956. Propagation of elastic waves in cylindrical shells including the effects of transverse shear and rotary inertia, Acoustical Sc. America 28(1): 56-63.
3. **Mirsky, I.; Hermann, G.** 1958. Axially motions of thick cylindrical shells, Appl. Mech. 25: 97-102.
4. **Yamanouchi, M.; Koizumi, M.; Shiota, I.** 1990. Proceedings of the first international symposium on functionally gradient materials, Sendai, Japan.
5. **Jabbari, M.; Sohrabpour, S.; Eslami, M.R.** 2002. Mechanical and thermal stresses in a functionally graded hollow cylinder due to radially symmetric loads, Int. J. Pres. Ves. Pip. 79: 493-497. http://dx.doi.org/10.1016/S0308-0161(02)00043-1.
6. **Chen, W.Q.; Lu, Y.; Ye, J.R.; Cai, J.B.** 2002. 3D electroelastic fields in a functionally graded piezoceramic hollow sphere under mechanical and electric loading, Arch. Appl. Mech. 72: 39-51. http://dx.doi.org/10.1007/s004190100184.
7. **Liu, X.; Wang, Q.; Quek, S.T.** 2002. Analytical solution for free vibration of piezoelectric coupled moderately thick circular plates, Int. J. Solid. Struct. 39: 2129-2151. http://dx.doi.org/10.1016/S0020-7683(02)00081-1.
8. **Wu, L.; Jiang, Z.; Liu, J.** 2005. Thermoelastic stability of functionally graded cylindrical shells, Compos. Struct. 70: 60-68. http://dx.doi.org/10.1016/j.compstruct.2004.08.012.
9. **Shi, Z.; F. Chen, Y.** 2004, Functionally graded piezoelectric cantilever beam under load, Arch. Appl. Mech. 74: 237-247.
10. **Peng-Fei, H.; Andrew, Y.T.** 2004. The transient responses of magneto-electro- elastic hollow cylinders, Smart. Mater, Struct. 13: 762-776. http://dx.doi.org/10.1088/0964-1726/13/4/014.
11. **Lu, P.; Lee, H.P.; Lu, C.** 2005. An exact solution for functionally graded piezoelectric laminated in cylindrical bending, Int. J. Mech. Sci. 47: 437-458. http://dx.doi.org/10.1016/j.ijmecsci.2005.01.012.
12. **Dai, H.L.; Fu, Y.M.; Yang, J.H.** 2007. Electromagnetoelastic behaviors of functionally graded piezoelectric solid cylinder and sphere, Acta. Mech. Solida. Sinica. 23: 55-63. http://dx.doi.org/10.1007/s10409-006-0047-0.
13. **Babaei, M.H.; Chen, Z.T.** 2008. Exact solutions for radially polarized and magnetized magnetoelectroelastic rotating cylinders, Smart. Mater. Struct. 17:025035, 11p.
14. **Jabbari, M.; Bahtui, A.; Eslami, M.R.** 2009. Axisymmetric mechanical and thermal stresses in thick short length FGM cylinders. Int. J. Pres. Ves. Pip. 86(5): 296-306. http://dx.doi.org/10.1016/j.ijpvp.2008.12.002.
15. **Khoshgoftar, M.J.; G. Arani, A.; Arefi, M.** 2009. Thermoelastic analysis of a thick walled cylinder made of functionally graded piezoelectric material. Smart. Mater. Struct. 18: 115007 . http://dx.doi.org/10.1088/0964-1726/18/11/115007.
16. **Arefi, M.; Rahimi, G.H.** 2010, Thermo elastic analysis of a functionally graded cylinder under internal pressure using first order shear deformation theory, Sci. Res. Essays 5(12): 1442-1454.
17. **Sheng, G.G., Wang, X.** 2010, Response and control of functionally graded laminated piezoelectric shells under thermal shock and moving loadings, Compos. Struct. 93: 132-141. http://dx.doi.org/10.1016/j.compstruct.2010.06.007.

18. **Sheng, G.G.; Wang, X.** 2010, Thermoelastic vibration and buckling analysis of functionally graded piezoelectric cylindrical shells. Appl. Math. Modelling 34: 2630-2643. http://dx.doi.org/10.1016/j.apm.2009.11.024.
19. **Dai, H.L.; Hong, L.; Fu, Y.M.; Xiao, X.,** 2010. Analytical solution for electromagnetothermoelastic behaviors of a functionally graded piezoelectric hollow cylinder, Appl. Math. Modelling. 34: 343-357. http://dx.doi.org/10.1016/j.apm.2009.04.008.
20. **Ghannad, K.M.; Rahimi, G.H.; EsmaeIlzadeh, Kh.S.** 2008. General plane elasticity solution of axisymmetric functionally graded thick cylindrical shell, Technical and Engineering Journal of Modares (in Persian).
21. **Ghannad, K.M., Rahimi, G.H.; EsmaeIlzadeh, Kh.S.** 2008. General shear deformation of axisymmetric functionally graded thick cylindrical shell, Technical and Engineering Journal of Modares (in Persian).
22. **Z. Nejad, M.; Rahimi, G.H.; Ghannad, K.M.** 2009. Set of field equations for thick shell of revolution made of functionally graded materials in curvilinear coordinate system, Mechanika 3(77): 18-26.
23. **Ghannad, M.; Z. Nejad, M.; Rahimi, G.H.** 2009. Elastic solution of axisymmetric thick truncated conical shells based on first-order shear deformation theory, Mechanika 5(79): 13-20.
24. **Arefi, M.; Rahimi, G.H.** 2011. Comprehensive thermoelastic analysis of a functionally graded cylinder with different boundary conditions under internal pressure using first order shear deformation theory, Mechanika (accepted for publication).
25. **Rahimi, G.H.; Arefi, M.; Khoshgoftar, M.J.** 2011. Application and analysis of functionally graded piezoelectrical rotating cylinder as mechanical sensor subjected to pressure and thermal loads, Appl. Math. Mech. (Engl. Ed) 32(8): 1-12 (In Press).
26. **Arefi, M.; Rahimi, G.H.** 2011. Three dimensional multi field equations of a functionally graded piezoelectric thick shell with variable thickness, curvature and arbitrary nonhomogeneity, Acta Mech, (In Press).

G. H. Rahimi, M. Arefi, M. J. Khoshgoftan

HERMETIŠKŲ STORASIENIŲ FUNKCIŠKAI KOKYBIŠKŲ PJEZOELEKTRINIŲ CILINDRŲ ELEKTRIŠKAI TAMPRI ANALIZĖ REMIANTIS PIRMOS EILĖS ŠLYTIES DEFORMACIJOS TEORIJA IR ENERGETINIU METODU

R e z i u m ė

Šlyties deformacijos teorija yra panaudota funkciškai kokybiško pjezoelektrinio cilindro, kaip vidinio slėgio nustatymo ir kontrolės fizikinio jutiklio, elektriškai tampriai analizei. Išskyrus Puasono koeficientą, visos mechaninės ir elektrinės charakteristikos yra išdėstytos polinėje koordinačių sistemoje. Preliminarus tyrimas atliktas remiantis šlyties deformacijos teorija kaip patikimesne ir pranašesne už plokščiąją tamprumo teoriją. Dvi radialinės ir ašinės deformacijos yra modeliuojamos remiantis pirmos eilės šlyties deformacijos teorija. Elektrinis potencialas yra pavaizduotas kvadratine funkcija sienelės storio kryptimi ir nežinoma funkcija – išilgine kryptimi. Nuo vamzdžio galų tolimų zonų tyrimo rezultatų palyginimas su remiantis plokščiąja tamprumo teorija gautais rezultatais patvirtina šio metodo tikslumą ir galimybes. Pateikti kai kurie naudingi grafiniais ir skaitiniais būdais gauti rezultatai. Aprašyta problema gali būti naudinga atliekant mechaninių ir elektrinių komponentų iš funkciškai kokybiškos medžiagos, naudojamos vietoj izotropinės, matavimus ir kontrolę.

G.H. Rahimi, M. Arefi, M.J. Khoshgoftar

ELECTRO ELASTIC ANALYSIS OF A PRESSURIZED THICK-WALLED FUNCTIONALLY GRADED PIEZOELECTRIC CYLINDER USING THE FIRST ORDER SHEAR DEFORMATION THEORY AND ENERGY METHOD

S u m m a r y

Shear deformation theory is employed for electro elastic analysis of a functionally graded piezoelectric cylinder as a physical sensor for estimation and controlling the internal pressure. Except Poisson ratio, all mechanical and electrical properties are graded along the radial coordinate system. The present paper develops the previous study using the shear deformation theory as a capable and advantageous theory instead of plane elasticity theory. Two radial and axial deformations are simulated using the first order shear deformation theory. Electric potential is supposed as a quadratic function along the thickness direction and as an unknown function along the longitudinal direction. Comparison between the present results at the regions that are adequate far from two ends of the cylinder with the results of plane elasticity theory justifies accuracy and capability of the present method. Some useful graphical and numerical results are presented in this study. The discussed problem in this paper has many advantageous properties and application in measurement and controlling of the mechanical and electrical components because of using the functionally graded materials instead of an isotropic material.

Keywords: electro elastic analysis, functionally graded piezoelectric cylinder, first order shear deformation theory, energy method.

Received March 03, 2011
Accepted May 30, 2012